ACADEMIC PRESS

Available online at www.sciencedirect.com

SCIENCE DIRECT®

Journal of Sound and Vibration 260 (2003) 763–775

JOURNAL OF SOUND AND VIBRATION

www.elsevier.com/locate/jsvi

Letter to the Editor

Natural frequencies of a flexible spinning disk misaligned with the axis of rotation

Jintai Chung*, Jin Wook Heo, Chang Soo Han

Department of Mechanical Engineering, Hanyang University, 1271 Sa-1-dong, Ansan, Kyunggi-do 425-791, South Korea

Received 7 May 2002; accepted 17 July 2002

1. Introduction

Spinning disks are widely used in optical disk and hard disk drives to store text, audio, image or video information. As the disk drives increasingly require faster data processing rates and higher recording density, vibration becomes one of main issues to be resolved in developing reliable disk drives. In particular, optical disk drives such as CD-R, CD-RW or DVD drives have an additional vibration source due to the misalignment between the axis of symmetry and the axis of rotation, compared to hard disk drives. Since most of the hard disks are precisely assembled with a spindle by a rigid clamp and they are not removed during its lifetime, the misalignment in the hard disk drives does not attract attention. However, the optical disks are removable and fixed by a magnetic clamp, so the axis of symmetry does not always coincide with the axis of rotation.

Since Southwell et al. [1,2] initiated a study on the vibration of a spinning disk, many researchers have been interested in the vibration of spinning disks. Among them, several papers were presented for imperfect spinning disks. Parker and Mote [3] analyzed the free vibration of coupled, asymmetric disk–spindle systems in which both the disk and spindle are continuous and flexible. Furthermore, Parker and Mote [4] presented a perturbation solution to predict natural frequencies of stationary annular or circular plates with slight deviation from axisymmetry and they discussed the mode split of the repeated natural frequencies. The transverse free and forced vibrations of a spinning circular disk with rectangular orthotropy were studied by Phylactopoulos and Adams [5,6]. They found that anisotropy of material caused the natural frequencies corresponding to cosine and sine normal modes to split. Recently, Kim et al. [7] reported that significant changes could occur to the natural frequencies and modes when a structure deviates from axisymmetry because of circumferentially varying model features. In addition, Chang and Wickert [8] investigated the forced vibration of a rotationally periodic structure when subjected to travelling wave excitation. Related to optical disks, on the other hand, Chung et al. [9] studied non-linear dynamic responses for a flexible spinning disk with angular acceleration.

*Corresponding author. Tel.: +82-31-400-5287; fax: +82-31-406-5550.
E-mail address: jchung@hanyang.ac.kr (J. Chung).

PII: S0022-460X(02)01078-7

In this paper, vibration characteristics of a flexible spinning disk are analyzed when the axis of symmetry is misaligned with the axis of rotation. With the assumption that the in-plane displacements are in a steady state and the out-of-plane displacement is in a dynamic state, the equations of both the in-plane and out-of-plane motions are derived from Hamilton's principle. From the equations of the in-plane motion, the exact solutions for the in-plane displacements are obtained. Then, by putting the exact solutions into the equation of the out-of-plane motion, a linear equation of motion is obtained for the out-of-plane displacement. This linear equation is discretized by using the Galerkin method. With the discretized equations, namely, the ordinary differential equation with respect to time, the effects of misalignment are investigated on the natural frequencies, mode shapes and critical speed of a spinning disk.

2. Equations of motion

Consider a flexible spinning annular disk with constant angular speed Ω, in which the axis of symmetry, C, is misaligned with the axis of rotation, O, as shown in Fig. 1. The amount of misalignment is given by distance ε between points C and O. The flexible spinning disk with thickness h, mass density ρ, Young's modulus E and the Poisson ratio v is homogeneous so that the centroid and the centre of mass are the same. The spinning disk is clamped at the inner radius $r = a$ by a rigid clamp and is free at the outer radius $r = b$. The motion of the disk, in this study, is described by the xyz-co-ordinate system that is fixed and rotating with the disk. Therefore, this xyz-co-ordinate frame is called the rotating frame of reference or the body-fixed frame of reference. In Fig. 1, the x-axis coincides with the extension of line OC, and the θ-co-ordinate is measured with respect to the x-axis. Since the xyz-co-ordinate system is fixed at the disk, the unit vectors $\mathbf{e}_r$ and $\mathbf{e}_\theta$ rotates along with the disk.

Denote the displacements in the r, θ and z directions by u, v, and w, respectively. Since the displacements u, v, and w are no longer axisymmetric due to misalignment ε, they are functions of the r- and θ-co-ordinates. Assuming that the in-plane displacements u and v are in a steady state

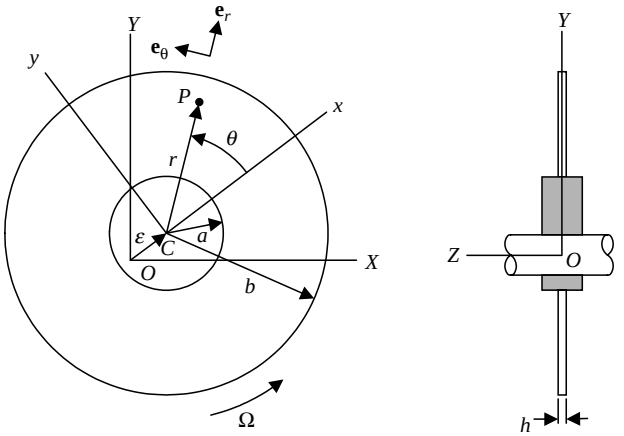

Fig. 1. Schematics of a spinning annular disk with misalignment.

while the out-of-plane displacement w is in a dynamic state, the displacements can be assumed as

$$u = u(r,\theta), \quad v = v(r,\theta), \quad w = w(t,r,\theta). \tag{1}$$

The equations of motion and the associated boundary conditions for the misaligned disk can be derived from Hamilton's principle. During deriving the equations of motion, the disk is assumed as the Kirhhoff plate and the in-plane inertia effects are neglected. Therefore, the equations for the in-plane displacement u and v are, strictly speaking, equations of in-plane stress equilibrium. The equations of motion for a spinning disk without misalignment can be found in some Refs. [10,11]. When the spinning disk has misalignment, the equations of motion may be represented as

$$\frac{\partial q_r}{\partial r} + \frac{\partial q_{r\theta}}{r\partial\theta} + \frac{q_r - q_\theta}{r} = -\rho h\Omega^2(r + \varepsilon\cos\theta), \tag{2}$$

$$\frac{\partial q_\theta}{r\partial\theta} + \frac{\partial q_{r\theta}}{\partial r} + 2\frac{q_{r\theta}}{r} = \rho h\varepsilon\Omega^2\sin\theta, \tag{3}$$

$$\rho h\frac{\partial^2 w}{\partial t^2} + D\nabla^4 w - \frac{\partial}{r\partial r}\left[r\left(q_r\frac{\partial w}{\partial r} + q_{r\theta}\frac{\partial w}{r\partial\theta}\right)\right] - \frac{\partial}{r\partial\theta}\left(q_\theta\frac{\partial w}{r\partial\theta} + q_{r\theta}\frac{\partial w}{\partial r}\right) = 0, \tag{4}$$

where q_r and q_θ are the radial and tangential membrane stresses, $q_{r\theta}$ is the shear membrane stress, D is the bending rigidity of the disk, and ∇^2 is the bi-harmonic operator:

$$q_r = \frac{Eh}{1-\nu^2}\left[\frac{\partial u}{\partial r} + \nu\left(\frac{u}{r} + \frac{\partial v}{r\partial\theta}\right)\right], \quad q_\theta = \frac{Eh}{1-\nu^2}\left(\nu\frac{\partial u}{\partial r} + \frac{u}{r} + \frac{\partial v}{r\partial\theta}\right)$$
$$q_{r\theta} = \frac{Eh}{2(1+\nu)}\left(\frac{\partial u}{r\partial\theta} + \frac{\partial v}{\partial r} - \frac{v}{r}\right), \tag{5}$$

$$D = \frac{Eh^3}{12(1-\nu^2)}, \quad \nabla^2 = \frac{\partial^2}{\partial r^2} + \frac{\partial}{r\partial r} + \frac{\partial^2}{r^2\partial\theta^2}. \tag{6}$$

Since the spinning disk is fixed at $r = a$ and free at $r = b$, the associate boundary conditions are given by

$$u = 0, \quad v = 0, \quad w = 0, \quad \frac{\partial w}{\partial r} = 0 \quad \text{at } r = a, \tag{7}$$

$$q_r = 0, \quad q_{r\theta} = 0, \quad m_r = 0 \quad \text{at } r = b, \tag{8}$$

$$-D\frac{\partial\nabla^2 w}{\partial r} + \frac{\partial m_{r\theta}}{r\partial\theta} = 0 \quad \text{at } r = b, \tag{9}$$

where

$$m_r = -D\left[\frac{\partial^2 w}{\partial r^2} + \nu\left(\frac{\partial w}{r\partial r} + \frac{\partial w}{r^2\partial\theta}\right)\right], \quad m_{r\theta} = -(1-\nu)D\left(\frac{\partial^2 w}{r\partial r\partial\theta} - \frac{\partial w}{r^2\partial\theta}\right). \tag{10}$$

It is interesting to see what happens in the equations of motion if misalignment ε equals zero. When $\varepsilon = 0$, the radial displacement u becomes a function of only r and the tangential displacement v becomes zero. Hence, q_r and q_θ become functions of only r and $q_{r\theta}$ becomes zero.

In this case, Eq. (3) is satisfied automatically and Eq. (2) reduces to

$$r^2\frac{d^2u}{dr^2}+r\frac{du}{dr}-u=-\frac{1-\nu^2}{E}\rho\Omega^2r^3, \tag{11}$$

which is the same as the conventional static equation of the in-plane motion for a spinning disk [12]. On the other hand, it is valuable to check that Eq. (4) is transformed into the equation governing the motion of the disk in the stationary frame of reference by using the relation

$$\phi=\theta-\Omega t, \tag{12}$$

where ϕ is measured counter-clockwise from the X-axis of the stationary frame of Ref. [10].

3. In-plane displacements

The exact solutions for the in-plane displacements are obtained from Eqs. (2) and (3). Since the steady state equations are dependent on only r and θ regardless of t and the in-plane displacements u and v are periodic with respect to θ, the in-plane displacements can be represented by an infinite series of the basis functions, i.e.,

$$u(r,\theta)=\sum_{j=0}^{\infty}[U_j(r)\cos j\theta+\bar{U}_j(r)\sin j\theta],\quad v(r,\theta)=\sum_{j=1}^{\infty}[V_j(r)\sin j\theta+\bar{V}_j(r)\cos j\theta]. \tag{13}$$

Substitution of Eqs. (13) into Eqs. (2) and (3) leads to the fact that the series solutions can be simplified as

$$u(r,\theta)=U_0(r)+U_1(r)\cos\theta,\quad v(r,\theta)=V_1(r)\sin\theta \tag{14}$$

because the right sides of Eqs. (2) and (3) have only $\cos\theta$ and $\sin\theta$, respectively. Furthermore, Eqs. (2) and (3) governing the in-plane motion may be expressed in terms of U_0, U_1 and V_1:

$$r^2\frac{d^2U_0}{dr^2}+r\frac{dU_0}{dr}-U_0=-\frac{1-\nu^2}{E}\rho\Omega^2r^3, \tag{15}$$

$$r^2\frac{d^2U_1}{dr^2}+r\frac{dU_1}{dr}+\frac{1+\nu}{2}r\frac{dV_1}{dr}-\frac{3-\nu}{2}U_1-\frac{3-\nu}{2}V_1=-\frac{1-\nu^2}{E}\rho\varepsilon\Omega^2r^2, \tag{16}$$

$$\frac{1-\nu}{2}r^2\frac{d^2V_1}{dr^2}-\frac{1+\nu}{2}r\frac{dU_1}{dr}+\frac{1-\nu}{2}r\frac{dV_1}{dr}-\frac{3-\nu}{2}U_1-\frac{3-\nu}{2}V_1=\frac{1-\nu^2}{E}\rho\varepsilon\Omega^2r^2. \tag{17}$$

The associated boundary conditions for Eqs. (15)–(17) are given by

$$U_0=U_1=V_1=0\quad\text{at } r=a, \tag{18}$$

$$\frac{dU_0}{dr}+\nu\frac{U_0}{r}=0\quad\text{at } r=b, \tag{19}$$

$$\frac{dU_1}{dr}+\nu\frac{U_1+V_1}{r}=0\quad\text{at } r=b, \tag{20}$$

$$\frac{dV_1}{dr}-\frac{U_1+V_1}{r}=0\quad\text{at } r=b. \tag{21}$$

It is noted that, if U_0 is replaced by u, Eq. (15) is identical to Eq. (11). This equation is an equation for the steady state radial displacement of the spinning disk when the disk has no misalignment. That is, U_0 is the radial displacement due to the centrifugal force. On the other hand, Eqs. (16) and (17) govern the radial and tangential displacements U_1 and V_1, which are generated by misalignment ε. If the misalignment is zero, then it is trivial that U_1 and V_1 become zero.

Consider how to derive the exact solutions for the equations of the in-plane motion given by Eqs. (15)–(17), with the boundary conditions given by Eqs. (18)–(21). The exact solution U_0 of Eq. (14) with the associated boundary conditions is well known. This solution is given by

$$U_0(r) = \frac{1-\nu^2}{8E}\rho\Omega^2\left[\frac{(1-\nu)a^4+(3+\nu)b^4}{(1-\nu)a^2+(1+\nu)b^2}\,r + \frac{(1+\nu)a^2-(3+\nu)b^2}{(1-\nu)a^2+(1+\nu)b^2}\frac{a^2b^2}{r} - r^3\right]. \tag{22}$$

Since Eqs. (16) and (17) are coupled by U_1 and V_1, it is necessary to rewrite them in matrix–vector form in order to obtain the exact solutions for U_1 and V_1:

$$r^2\begin{bmatrix}2 & 0\\ 0 & 1-\nu\end{bmatrix}\frac{\mathrm{d}^2}{\mathrm{d}r^2}\begin{Bmatrix}U_1\\ V_1\end{Bmatrix} + r\begin{bmatrix}2 & 1+\nu\\ -1-\nu & 1-\nu\end{bmatrix}\frac{\mathrm{d}}{\mathrm{d}r}\begin{Bmatrix}U_1\\ V_1\end{Bmatrix} - (3-\nu)\begin{bmatrix}1 & 1\\ 1 & 1\end{bmatrix}\begin{Bmatrix}U_1\\ V_1\end{Bmatrix} = \frac{2(1-\nu^2)}{E}\rho\varepsilon\Omega^2 r^2\begin{Bmatrix}-1\\ 1\end{Bmatrix}. \tag{23}$$

According to the method of Frobenius [13], the homogeneous solution of Eq. (23) is assumed as

$$\begin{Bmatrix}U_1\\ V_1\end{Bmatrix}_H = r^\lambda\begin{Bmatrix}c_H\\ d_H\end{Bmatrix} \tag{24}$$

and the particular solution is assumed as

$$\begin{Bmatrix}U_1\\ V_1\end{Bmatrix}_P = r^2\begin{Bmatrix}c_P\\ d_P\end{Bmatrix}. \tag{25}$$

The homogeneous and particular solutions for U_1 and V_1 are easily determined by substituting Eqs. (24) and (25) into Eq. (23). Summation of the homogeneous and particular solutions yields the general solutions for U_1 and V_1. By applying the boundary conditions of Eqs. (18)–(21) to the general solutions, the displacements due to the misalignment can be represented by

$$\begin{aligned} U_1(r) &= \frac{1+\nu}{8E}\rho\varepsilon\Omega^2\left(c_1r^2 + \frac{c_2}{r^2} + c_3\ln\frac{r}{a} + c_4\right),\\ V_1(r) &= \frac{1+\nu}{8E}\rho\varepsilon\Omega^2\left(d_1r^2 + \frac{d_2}{r^2} + d_3\ln\frac{r}{a} + d_4\right), \end{aligned} \tag{26}$$

where

$$c_1 = -\frac{8(1-\nu)a^4-(1+\nu)(1-3\nu)a^2b^2+3(1-\nu^2)b^4}{(3-\nu)a^4+(1+\nu)b^4},$$

$$c_2 = \frac{(1+\nu)[(1-\nu)a^2+(1+\nu)b^2]}{(3-\nu)a^4+(1+\nu)b^4}a^2b^4,$$

$$d_1 = -c_1 + \frac{2(1+\nu)[(3-\nu)a^2 - (1-\nu)b^2]}{(3-\nu)a^4 + (1+\nu)b^4}b^2, \quad d_2 = c_2, \quad d_3 = -c_3,$$
$$d_4 = -c_4 - 2(1+\nu)b^2. \tag{27}$$

Meanwhile, the membrane stresses, namely, the in-plane stresses can be expressed in terms of U_0, U_1 and V_1. These membrane stresses may be rewritten as

$$q_r(r,\theta) = Q_r^{(0)}(r) + Q_r^{(1)}(r)\cos\theta, \quad q_\theta(r,\theta) = Q_\theta^{(0)}(r) + Q_\theta^{(1)}(r)\cos\theta,$$
$$q_{r\theta}(r,\theta) = Q_{r\theta}^{(1)}(r)\sin\theta, \tag{28}$$

where $Q_r^{(0)}$ and $Q_\theta^{(0)}$ are the stresses due to the centrifugal force while$Q_r^{(1)}$, $Q_\theta^{(1)}$ and $Q_{r\theta}^{(1)}$ are the stresses due to the misalignment at a given θ:

$$Q_r^{(0)}(r) = \frac{Eh}{1-\nu^2}\left(\frac{\mathrm{d}U_0}{\mathrm{d}r} + \nu\frac{U_0}{r}\right), \quad Q_\theta^{(0)}(r) = \frac{Eh}{1-\nu^2}\left(\nu\frac{\mathrm{d}U_0}{\mathrm{d}r} + \frac{U_0}{r}\right),$$
$$Q_r^{(1)}(r) = \frac{Eh}{1-\nu^2}\left(\frac{\mathrm{d}U_1}{\mathrm{d}r} + \nu\frac{U_1+V_1}{r}\right), \quad Q_\theta^{(1)}(r) = \frac{Eh}{1-\nu^2}\left(\nu\frac{\mathrm{d}U_1}{\mathrm{d}r} + \frac{U_1+V_1}{r}\right),$$
$$Q_{r\theta}^{(1)}(r) = \frac{Eh}{2(1+\nu)}\left(\frac{\mathrm{d}V_1}{\mathrm{d}r} - \frac{U_1+V_1}{r}\right). \tag{29}$$

4. Out-of-plane motion

The Galerkin method is used to obtain discretized equations from the equation of the out-of-plane motion given by Eq. (4). The out-of-plane displacement w can be approximated by

$$w(t,r,\theta) = \sum_{m=0}^{M}\sum_{n=0}^{N} W_{mn}(r)[C_{mn}(t)\cos n\theta + S_{mn}(t)\sin n\theta], \tag{30}$$

where M and N are the numbers of the basis functions used in approximation of the radial and tangential contributions respectively; W_{mn} is a basis function for the radial direction; C_{mn} and S_{mn} are functions of time. The basis function W_{mn} should be the comparison function, which satisfies both the essential and natural boundary conditions. The radial basis function W_{mn} can be chosen as

$$W_{mn}(r) = (r-a)^{m+2}(a_{mn} + b_{mn}r + c_{mn}r^2), \tag{31}$$

where a_{mn}, b_{mn} and c_{mn} are constants to be determined by the natural boundary conditions and the normalization condition. Applying the Galerkin method with Eq. (30), discretized equations can be written in matrix–vector form

$$\mathbf{M}\ddot{\mathbf{T}} + \left(\mathbf{K}^b + \mathbf{K}^p\right)\mathbf{T} = 0, \tag{32}$$

where the superposed dots denote differentiation with respect to time; $\mathbf{M}$ is a mass matrix; $\mathbf{K}^b$ and $\mathbf{K}^p$ are the stiffness matrices due to the bending rigidity and the membrane stresses; $\mathbf{T}$ is a column vector that is a function of time.

The natural frequencies of the out-of-plane motion are investigated with Eq. (32). The material properties and dimensions used in the computations in this paper, if there is no other remark, are given by $a = 15\,\text{mm}$, $b = 65\,\text{mm}$, $h = 1.2\,\text{mm}$, $\rho = 1200\,\text{kg/m}^3$, $E = 65.5 \times 10^6\,\text{N/m}^2$ and $v = 0.3$. This data is for a conventional optical disk, e.g., a CD-ROM disk. The natural frequencies can be computed from

$$(\mathbf{K}^b + \mathbf{K}^p - \omega_n^2\mathbf{M})\mathbf{X} = \mathbf{0}, \tag{33}$$

where ω_n is the natural frequency in the rotating frame of reference and $\mathbf{X}$ is the corresponding normal mode vector.

A convergence test for the natural frequencies is carried out when Ω and ε are not equal to zero. The convergence of the natural frequencies of a disk with $a/b = \frac{3}{13}$, when Ω=1000 rad/s and $\varepsilon/b = 0.2$, is presented in Table 1, which shows that the natural frequencies converge with M. In Table 1, the mode (m, n) represents a mode with m nodal circles and n nodal diameters. An interesting phenomenon observed in Table 1 is the fact that the modes (0, 1), (0, 2) and (0, 3) have two natural frequencies. When there is no misalignment in a disk, all the modes possess only one natural frequency in the rotating frame of reference. However, when the disk has misalignment, the natural frequency for the mode (m, n) where $n \neq 0$ is split into two frequencies: the one is for the symmetric mode and the other is for the asymmetric mode. The subscripts s and a in Table 1 stand for the symmetric and asymmetric modes, respectively. The symmetric mode is symmetric with respect to the x-axis of Fig. 1 while the asymmetric mode is not symmetric. The misalignment in a disk plays a role of deviation from axisymmetry. More detailed discussions about the symmetric and asymmetric modes, which are sometimes called sine and cosine modes, can be found in Refs. [5–8,14].

Next, the natural frequencies of a spinning are investigated for the spinning speed when misalignment exists. Fig. 2 presents the variation of the natural frequencies for the spinning speed in the rotating frame of reference when $a/b = \frac{3}{13}$ and $\varepsilon/b = 0.2$. Similar to the natural frequencies for a disk without misalignment, all the frequencies monotonically increase with the spinning speed. As pointed out above, the natural frequency of the mode (m, n) where $n \neq 0$ split into two frequencies when the spinning speed is not equal to zero. Fig. 2 shows that the natural frequency corresponding to the (0, 1) mode is split into the frequencies for the symmetric mode $(0, 1)_s$ and the asymmetric mode $(0, 1)_a$. However, since the natural frequencies of the symmetric and asymmetric

Table 1
Convergence characteristics of the natural frequencies (rad/s) in the rotating frame of reference when $a/b = 3/13$, $\Omega = 1000\,\text{rad/s}$ and $\varepsilon/b = 0.2$

M	Mode						
	$(0,0)$	$(0,1)_s$	$(0,1)_a$	$(0,2)_s$	$(0,2)_a$	$(0,3)_s$	$(0,3)_a$
1	788.0536	1260.848	1132.911	1523.828	1524.110	1924.129	1925.393
2	773.5180	1243.861	1121.035	1515.237	1515.360	1917.959	1919.172
3	771.8546	1239.174	1118.751	1513.483	1513.717	1917.238	1918.478
4	761.4539	1239.013	1118.631	1513.410	1513.700	1917.124	1918.418
5	768.5637	1237.157	1116.963	1512.567	1512.903	1916.880	1918.205
6	768.1173	1234.892	1116.070	1511.835	1512.214	1916.768	1918.090
7	767.8218	1234.090	1115.989	1511.689	1512.136	1916.746	1918.082

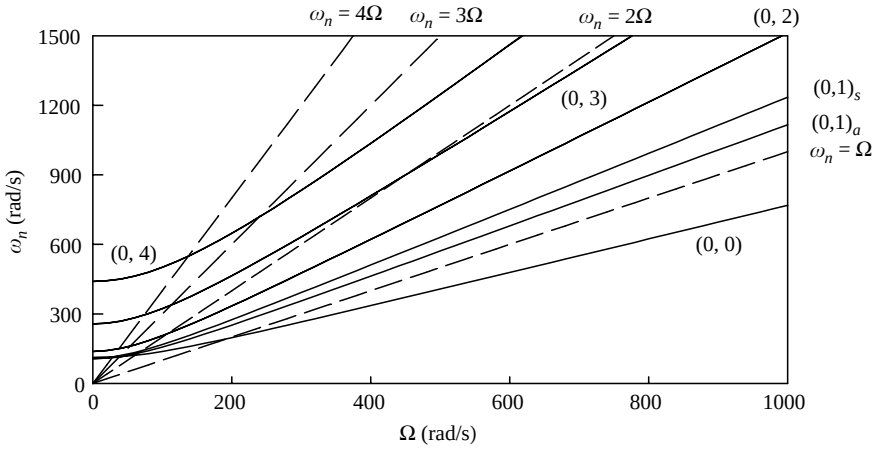

Fig. 2. Variation of the natural frequencies for the spinning speed in the rotating frame of reference when $a/b = 3/13$ and $e/b = 0.2$.

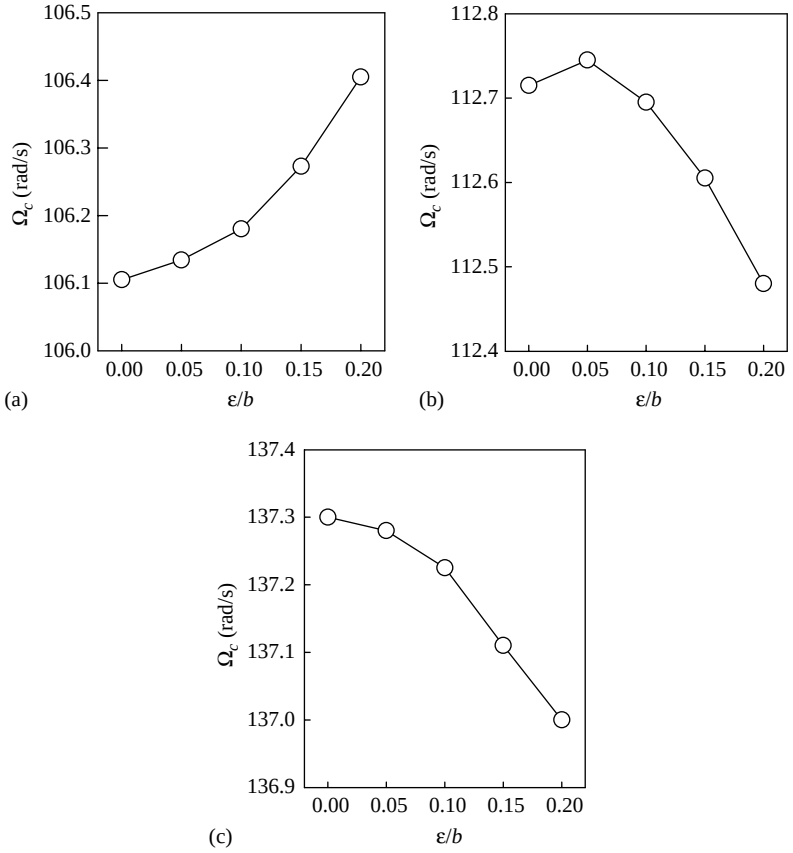

Fig. 3. Variation of the critical speed for the misalignment of a spinning disk with $a/b = 3/13$: (a) the $(0, 2)$ mode; (b) the $(0, 3)$ mode; and (c) the $(0, 4)$ mode.

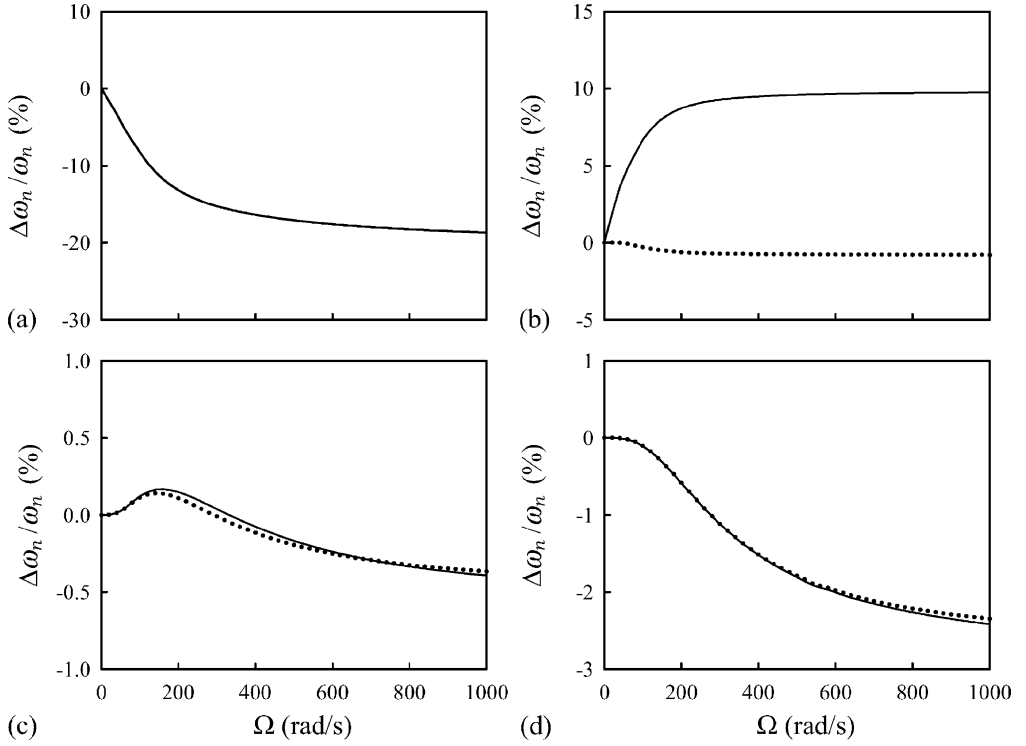

Fig. 4. Differences of the natural frequencies between when $\varepsilon/b = 0.2$ and when $\varepsilon/b = 0$ for the variation of the spinning speed: (a) the (0, 0) mode; (b) the (0, 1) modes; (c) the (0, 2) modes; and (d) the (0, 3) modes. ———, symmetric mode; ⋯, asymmetric mode.

modes have very small differences in the modes (0, 2), (0, 3) and (0, 4), they do not seem to be split into two frequencies.

The critical speeds of a disk are influenced by the misalignment. Denoting by λ_n the natural frequency computed in the stationary frame of reference, the relationship between λ_n and ω_n is given by

$$\lambda_n = \omega_n \pm n\Omega, \tag{34}$$

where n is the number of nodal diameters. The dashed lines in Fig. 2 represent lines corresponding to $\omega_n = n\Omega$. Note that the critical speed is defined by the spinning speed at which the natural frequency in the stationary frame of reference, λ_n, becomes zero. Therefore, it is inferred from Eq. (34) that the critical speed Ω_c is a value of Ω at which the line of $\omega_n = n\Omega$ intersects with the natural frequency curve of the (m, n) mode. However, the curve of the (0, 1) mode does not intersect with the line of $\omega_n = \Omega$, so there is no critical speed corresponding to the (0, 1) mode. Fig. 3 shows the variation of the critical speed for the misalignment when $a/b = \frac{3}{13}$. When the misalignment changes from $e \cdot b = 2$ to $e/b = 0.2$, the lowest critical speed, namely, the critical speed of the (0, 2) mode, increases from 106.105 to 106.405 rad/s.

To analyze the effects of misalignment on the natural frequencies in more detail, the differences of the natural frequencies between the disks with and without misalignment are investigated when

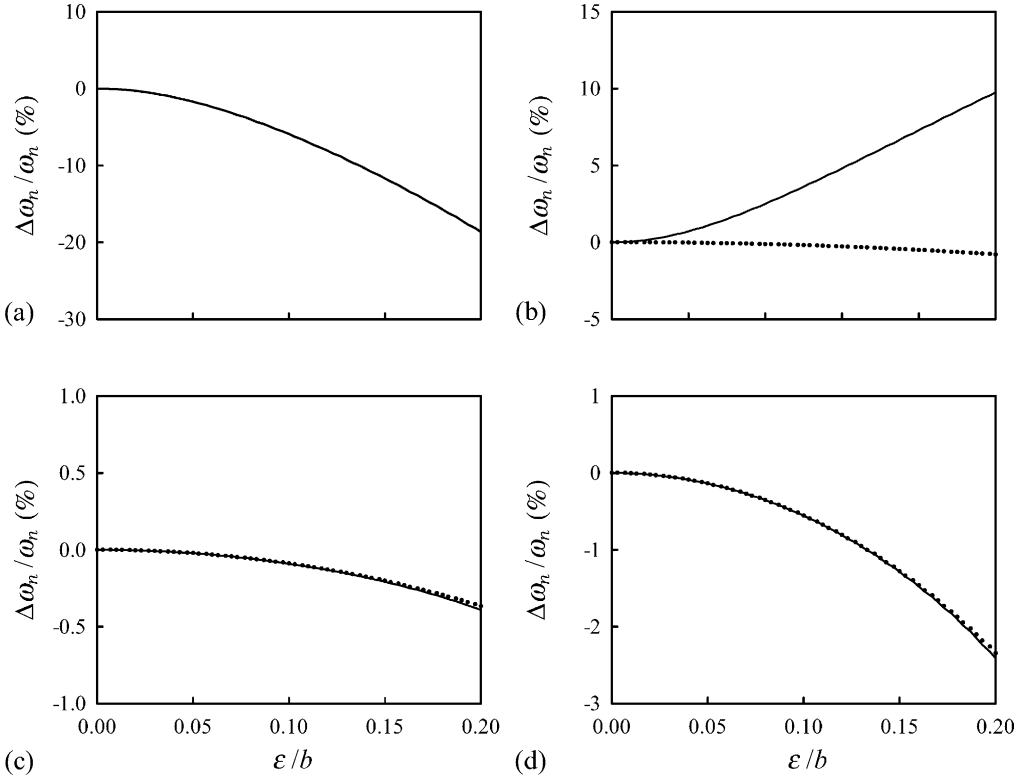

Fig. 5. Differences of the natural frequencies between when $\varepsilon/b = 0.2$ and when $\varepsilon/b = 0$ for the variation of misalignment: (a) the $(0, 0)$ mode; (b) the $(0, 1)$ modes; (c) the $(0, 2)$ modes; and (d) the $(0, 3)$ modes. ———, symmetric mode; ⋯, asymmetric mode.

$a/b = \frac{3}{13}$. Fig. 4 shows the ratios of $\Delta\omega_n = \omega_n(\varepsilon/b = 0.2) - \omega_n(\varepsilon/b = 0)$ to $\omega_n(\varepsilon/b = 0)$ versus the spinning speed while Fig. 5 shows the ratios of $\Delta\omega_n = \omega_n(\varepsilon/b \neq 0) - \omega_n(\varepsilon/b = 0)$ to $\omega_n(\varepsilon/b = 0)$ versus the misalignment. In Figs. 4 and 5, the solid and the dotted lines represent the symmetric and the asymmetric modes, respectively. It is observed in Figs. 4 and 5 that the $(0, 1)$ mode has larger differences between the symmetric and asymmetric modes compare to the other modes. It is also observed that these differences increase with the magnitude of the spinning speed and the amount of misalignment.

Finally, the effects of misalignment on the mode shapes of the spinning disk are studied when the disk with $a/b = \frac{3}{13}$ has a constant angular speed $\Omega = 1000$ rad/s. The mode shapes of the disk with misalignment $\varepsilon/b = 0.2$ are shown in Fig. 6, where it is observed that the $(0, 0)$ mode is distorted from an axisymmetric shape and the asymmetric modes $(0, n)_a$ rotate from symmetric modes $(0, n)_s$. In order to scrutinize variations of the mode shapes along the outer circumference, the mode shapes at the outer radius are presented as functions of the tangential coordinate θ in Fig. 7, where the solid and dotted lines represent the symmetric and asymmetric modes respectively. Fig. 7 shows that the mode shapes do not remain purely harmonic in the θ direction when the disk has misalignment. It is well known that an axisymmetric disk has purely harmonic mode shapes in the θ direction. Therefore, the misalignment plays a role of deviation from

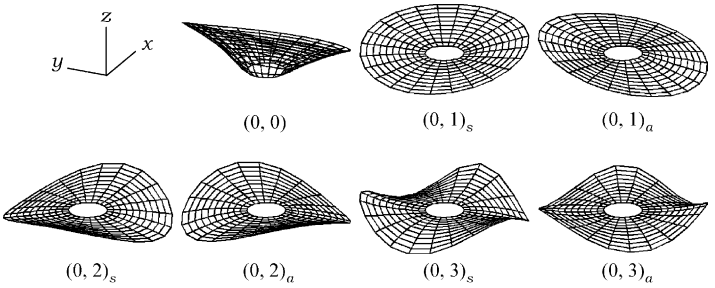

Fig. 6. Mode shapes of the spinning disk with misalignment $\varepsilon/b = 0.2$ when $a/b = 3/13$ and $\Omega = 1000$ rad/s.

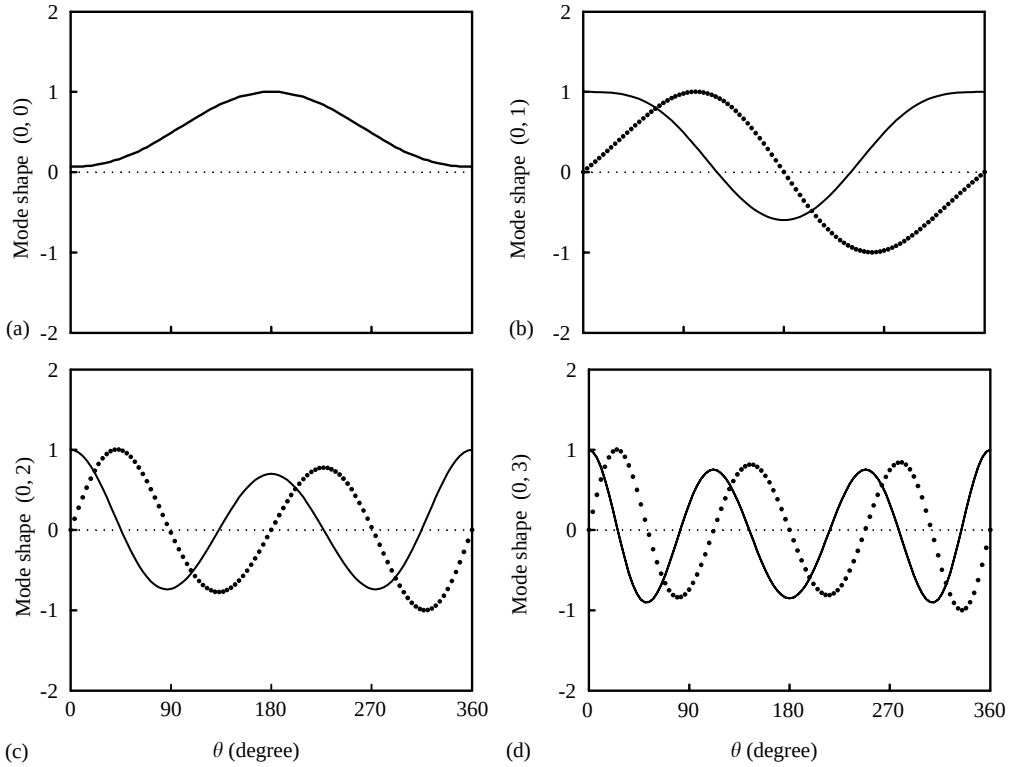

Fig. 7. Mode shapes of the spinning disk along the outer circumference when $\varepsilon/b = 0.2$, $a/b = 3/13$ and $\Omega = 1000$ rad/s: (a) the $(0,0)$ mode; (b) the $(0,1)$ modes; (c) the $(0,2)$ modes; and (d) the $(0,3)$ modes. ———, symmetric mode; ⋯, asymmetric mode.

axisymmetry. This distortion from purely harmonic mode shapes, which is often called the wave number contamination of modes was discussed by Kim et al. [7] and Chang and Wickert [8].

5. Conclusions

The equations of motion are derived for a spinning disk whose axis of symmetry is misaligned with the axis of rotation. Assuming that the in-plane motion of the disk is in a steady state and the

out-of-plane motion is in a dynamic state, the governing equations for both the in-plane and out-of-plane motions are derived from Hamilton's principle. The derived equations consist of two linear equations and a non-linear equation: the linear equations are for the in-plane motion and the non-linear equation is for the out-of-motion. After the exact solutions for the in-plane displacements are found, they are plugged into the non-linear equation of the out-of-plane motion to obtain a new linear equation.

Based upon the linear equation for the out-of-plane displacement, the natural frequencies and mode shapes of spinning disks with misalignment are studied. The results obtained from this study can be summarized as follows:

(1) When a disk has misalignment, a natural frequency for the mode (m, n) where $n \neq 0$ is split into two frequencies: a frequency for the symmetric mode and a frequency for the asymmetric mode.
(2) The $(0, 1)$ mode has larger difference between the frequencies of the symmetric and asymmetric modes than the other modes.
(3) The misalignment of a spinning disk results in distortion of the mode shapes, so called, the wave number contamination of modes.
(4) The lowest critical speed of a spinning disk increases with misalignment.

Acknowledgements

The authors are grateful for the financial support provided by a grant (Grant number: R01-2000-00292) from the Korea Science and Engineering Foundation (KOSEF).

References

[1] H. Lamb, R.V. Southwell, The vibration of a spinning disk, Proceedings of the Royal Society 99 (1921) 272–280.
[2] R.V. Southwell, On the free transverse vibrations of a uniform circular disc clamped at its centre; and on the effects of rotation, Proceedings of the Royal Society 101 (1922) 133–153.
[3] R.G. Parker, C.D. Mote, Vibration and coupling phenomena in asymmetric disk–spindle systems, American Society of Mechanical Engineers, Journal of Applied Mechanics 63 (1996) 953–961.
[4] R.G. Parker, C.D. Mote, Exact perturbation for the vibration of almost annular or circular plates, American Society of Mechanical Engineers, Journal of Vibration and Acoustics 118 (1996) 436–455.
[5] A. Phylactopoulos, G.G. Adams, Transverse vibration of a rectangularly orthotropic spinning disk, Part 1: formulation and free vibration, American Society of Mechanical Engineers, Journal of Vibration and Acoustics 121 (1999) 273–279.
[6] A. Phylactopoulos, G.G. Adams, Transverse vibration of a rectangularly orthotropic spinning disk, Part 2: forced vibration and critical speeds, American Society of Mechanical Engineers, Journal of Vibration and Acoustics 121 (1999) 280–285.
[7] M. Kim, J. Moon, J.A. Wickert, Spatial modulation of repeated vibration modes in rotationally periodic structures, American Society of Mechanical Engineers, Journal of Vibration and Acoustics 122 (2000) 62–68.
[8] J.Y. Chang, J.A. Wickert, Response of modulated doublet modes to travelling wave excitation, Journal of Sound and Vibration 242 (2001) 69–83.
[9] J. Chung, J.-E. Oh, H.H. Yoo, Non-linear vibration of a flexible spinning disc with angular acceleration, Journal of Sound and Vibration 231 (2000) 375–391.

[10] W.D. Iwan, T.L. Moeller, The stability of a spinning elastic disk with a transverse load system, American Society of Mechanical Engineers, Journal of Applied Mechanics 43 (1976) 485–490.
[11] S.G. Hutton, S. Chonan, B.F. Lehmann, Dynamic response of a guided circular saw, Journal of Sound and Vibration 112 (1987) 527–539.
[12] S. Timoshenko, J.N. Goodier, Theory of Elasticity, McGraw-Hill, New York, 1970.
[13] F.B. Hildebrand, Advanced Calculus for Applications, Prentice-Hall, Englewood Cliffs, NJ, 1976.
[14] J. Chung, J.M. Lee, Vibration analysis of a nearly axisymmetric shell structure using a new finite ring element, Journal of Sound and Vibration 219 (1999) 35–50.